Available online at www.eccomasproceedia.org
Eccomas Proceedia COMPDYN (2025) 721- 7

ECCOMAS
Proceedia

COMPDYN 2025
10th ECCOMAS Thematic Conference on
Computational Methods in Structural Dynamics and Earthquake Engineering
M. Papadrakakis, M. Fragiadakis (eds.)
Rhodes Island, Greece, 15-18 June 2025

FVDs AND HYSTERETIC STRUCTURES: DESIGN STRATEGIES

Anthea Amato[1, 2], **Liborio Cavaleri**[1], **Maria Concetta Oddo**[1]

[1] University of Palermo
Viale delle Scienze, Palermo, Italy
{ anthea.amato, liborio.cavaleri, mariaconcetta.oddo01}@unipa.it

[2] University of Catania
Piazza Università, Catania, Italy
anthea.amato@phd.unict.it

Abstract

Nowadays fluid viscous dampers (FVDs) are among the most used passive energy dissipation devices thanks to their capacity to generate velocity dependent dissipative forces, not in phase with the displacements, that exhibit their maximum value when internal restoring forces are minimum. Often preferred over other types of dampers, FVDs have also the advantage of increasing the damping ratio of structures without significantly altering the inherent stiffness. One of the issues, mostly connected to the structures exhibiting a nonlinear plastic behavior, despite the structures maintaining an elastic one, is the absence of specific code prescriptions and simple, but sufficiently reliable, design strategies. To overcome this lack could make the use of viscous dampers, characterized by a linear or, more generally, nonlinear velocity dependence of the dissipative forces, more diffused than it is. With the aim of simplifying the procedure for practical applications, a novel design strategy for nonlinear FVDs to apply to hysteretic reinforced concrete framed structures is proposed and discussed in terms of reliability, by analyzing the results in a statistical sense. An initial hypothesis, consisting of a simplified dynamic structural response assumed to be coupled to the equivalent linearization of FVDs, is necessary for this scope. To prove the suitability of this hypothesis, a comparison between the obtainable results and the design targets is carried out for those structures that do not satisfy the assumed hypothesis, through time history analyses performed on FVDs-equipped (and non) structural nonlinear models. Benchmark models, subjected to appropriate families of base accelerograms, are analyzed to test the procedure and its degree of success in connection to the assumed target objectives.

Keywords: Fluid Viscous Dampers, design strategy, hysteretic structures, seismic protection.

ISSN:2623-3347 Published by Eccomas Proceedia.
Peer-review under responsibility of the organizing committee of COMPDYN 2025.
doi: 10.7712/120125.12685.25626

1 INTRODUCTION

Design and distribution of FVDs, categorized as passive energy dissipation devices, are standardized in current codes by simplified approaches (e.g. FEMA 356 [1]): assuming structural damage dissipation as an equivalent damping inherent force or non-considering it at all by providing a viscous dissipation as great as possible to maintain the structure in an elastic stage [e.g. 2 and 3]. Since they have recently emerged as prominent solutions for mitigating the response of existing civil structures and infrastructures (while also limiting excessive internal forces or ductility demand [4–17]), maintaining the structure in an elastic stage could be expensive in case of retrofitting. Able to generate velocity dependent dissipative forces, not in phase with the displacements, exhibiting their maximum value when internal restoring forces are minimum (so the influence on the structural inherent stiffness is really contained [18]), to overcome the lack of effective solutions for practical applications could make the use of viscous dampers more diffused than it is. The issue is mostly related to those structures that exhibit a non linear behaviour since for new structures it is not a problem because FVDs' job is precisely to prevent hysteretic dissipation. So, the goal is that the structural response under earthquake excitation has to be contained by reducing the ductility demand and increasing the viscous damping provided by the added dampers, without renouncing to the inelastic energy dissipation capacity [19].

With the aim of simplifying the procedure for practical applications, a novel design strategy for FVDs to apply to hysteretic reinforced concrete framed structures is proposed: seismic energy dissipation is provided by inherent damping, fluid viscous additional damping and hysteretic behavior of structural members. Additionally, design of external viscous damping is conducted starting just from the rate of energy that the structure can dissipate by hysteretic damping, depending on a comparison between the actual ductility capacity of the structure (predicted by a pushover analysis) and the ductility demand obtained using the response spectra (of accelerations and displacements) in agreement to the method N2 [20]. This solution is really valuable for existing structures, being able to combine a limitation of the intervention cost (with the novelty of considering external viscous damping as complementary to the hysteretic structural capacity, since the latter is effective for the scope to limit the seismic response) and the advantages of the linear analysis approaches.

An initial hypothesis, consisting of a simplified dynamic structural response assumed to be coupled to the equivalent linearization of FVDs, is necessary for this scope. To prove the suitability of this hypothesis, a comparison between the obtainable results and the design targets is carried out for those structures that do not satisfy the assumed hypothesis, through time history analyses performed on FVDs-equipped (and non) structural nonlinear models. Benchmark models, subjected to appropriate families of base accelerograms, are analyzed to test the procedure and its degree of success in connection to the assumed target objectives.

2 FLUID VISCOUS DAMPERS' CONSTITUTIVE LAW

In Eq. (1) the damper force f_i exhibited by the damper located in the i-th interstorey is expressed as:

$$f_i = C_i \cdot \left| l_i \left(\dot{u}_i - \dot{u}_{i-1} \right) \right|^{\alpha} \cdot \operatorname{sgn}\left(\dot{u}_i - \dot{u}_{i-1} \right) = C_i l_i^{\alpha} \left| \left(\dot{u}_i - \dot{u}_{i-1} \right) \right|^{\alpha} \cdot \operatorname{sgn}\left(\dot{u}_i - \dot{u}_{i-1} \right) \tag{1}$$

The force is related to the $\operatorname{sgn}\left(\dot{u}_i - \dot{u}_{i-1} \right)$, "signum" function of the interstorey velocity, through C_i and α, parameters dependent on constructive damper properties, and l_i, that gives information about how dampers are installed (equal to 1 in the case of K support braces).

Observe that the increase of the parameter C_i is associated with an increase in the maximum force exhibited by an FVD. Further, the progressive reduction of the exponent α makes the cycle force-displacement exhibited by an FVD close to a rectangle (α=1 is associated to an elliptical cycle, when α=0 the force displacement cycle is a rectangle).

Once fluid viscous dampers are installed on a plane shear type system, the n-degrees-of-freedom govern equation changes, becoming:

$$\mathbf{M}\ddot{\mathbf{u}} + \mathbf{C}\dot{\mathbf{u}} + \mathbf{R}\left(\dot{\mathbf{u}}, \alpha\right) + \mathbf{F}\left(\mathbf{u}, \dot{\mathbf{u}}\right) = \mathbf{M}\boldsymbol{\tau}\ddot{u}_g \tag{2}$$

Showing a new component, **R**, that is a vector in which the forces exhibited in the fluid viscous dampers and transferred to each storey are contained, vector **F** contains the restoring hysteretic forces, **C** is the inherent damping matrix and $\boldsymbol{\tau}$ is the influence vector.

When α is equal to 1, ***R*** can be simply expressed as:

$$\mathbf{R}\left(\dot{\mathbf{u}}, \alpha = 1\right) = \tilde{\mathbf{C}}\mathbf{T}\dot{\mathbf{u}} \tag{3}$$

In Eq. (3), **T** is a nxn transformation diagonal matrix containing the transformation factor, while $\tilde{\mathbf{C}}$ is the matrix containing the constants (C_i) appearing in Eq (1).

3 THE PROPOSED STRATEGY

According to the N2 method, from a monotonic bilinear equivalent form of the F-δ curve, it is possible to obtain the available ductility of the system μ_a, to be compared with the demand in terms of ductility μ_d, expressed as follow:

$$\mu_a = \frac{\delta_{ua}}{\delta_e}, \quad \mu_d = \frac{\delta_{ud}}{\delta_e} \tag{4}$$

Since the denominator is the same, the comparison is between the ultimate displacement (δ_{ua}) and the corresponding demand (δ_{ud}). The strength reduction factor R_μ is:

$$R_\mu = \frac{mS_e(T^*)}{F_r} \tag{5}$$

In which F_r is the strength of the equivalent bilinear SDOF system, compared to the strength required for an elastic linear system (derived from the pseudo-acceleration response spectrum).

Depending on the natural period domain, T*, the displacement demand for an elastic linear system and for an elastic perfect plastic system characterized by a strength reduction factor R_μ are related as follows:

$$\begin{aligned} R_\mu &= \left(\frac{\delta_{ud}}{\delta_e} - 1\right)\frac{T^*}{T_C} + 1; \quad 0 \le T^* < T_C \\ R_\mu &= \frac{\delta_{ud}}{\delta_e}; \quad T^* \ge T_C \end{aligned} \tag{6}$$

Rewriting the latter equations, marking the dependence of $S_e(T^*)$ on the damping ratio ς, the only unknown is the damping ratio ς_{eff} corresponding to a ductility demand fixed equal to the ductility capacity:

$$\begin{aligned} \frac{mS_e(T^*,\varsigma_{eff})}{F_r} &= \left(\frac{\delta_{ua}}{\delta_e}-1\right)\frac{T^*}{T_C}+1; \quad 0 \le T^* < T_C \\ \frac{mS_e(T^*,\varsigma_{eff})}{F_r} &= \frac{\delta_{ua}}{\delta_e}; \quad T^* \ge T_C \end{aligned} \tag{7}$$

Solving Eqs. (7) means finding the best additional damping ratio expressed as a difference between the effective one and the inherent ratio of the structure in the state before the enhancement:

$$\varsigma_d = \varsigma_{eff} - \varsigma \tag{8}$$

Once obtained the best additional damping ratio it has to be related to an appropriate number and distribution of FVDs. To do this some hypotheses are taken into account: the structure has a plane shear type behaviour, dampers have a linear behaviour (namely characterized by α=1), even if α is generally not higher than 0.5, a uniform distribution of FVDs in elevation, dissipation capacity constant at each storey and defined by a scalar parameter C, the coincidence of the FVDs' velocity and the interstorey velocity. Under these hypotheses, Eq (2) can be rewritten as:

$$\mathbf{M}\ddot{\mathbf{u}}(t)+\mathbf{C}^{(S)}\dot{\mathbf{u}}(t)+\mathbf{C}^{(D)}\dot{\mathbf{u}}(t)+\mathbf{K}\mathbf{u}(t)=-\mathbf{M}\boldsymbol{\tau}\ddot{x}_g(t) \tag{9}$$

Where $\mathbf{C}^{(S)}$ is the structural inherent damping matrix and $\mathbf{C}^{(D)}$ is the damping matrix associated to the FVDs, that is:

$$\mathbf{C}^{(D)} = C \cdot \mathbf{P} \tag{10}$$

where P is the tridiagonal matrix, whose terms assume the following values P_{ii}:

$$P_{ii} = 2 \ \forall i \ne n; \ P_{nn} = 1; \ P_{ij} = -1 \ \forall j = i \pm 1 \tag{11}$$

In which n is the number of storeys.

The last simplification is that the structural response is assumed to be governed by the first eigenvector, $\boldsymbol{\phi}_1$, so that it is possible to write:

$$C = 2\xi_d\omega_1\frac{\boldsymbol{\phi}_1^T\mathbf{M}\boldsymbol{\phi}_1}{\boldsymbol{\phi}_1^T\mathbf{P}\boldsymbol{\phi}_1} \tag{12}$$

Representative of the dissipation provided by all the FVDs at one storey in one direction. Even if equivalent to the simplified formula proposed by FEMA 356 [1], ξ_d in Eq. (12) has a totally different meaning since it is the exact supplemental damping ratio needed for a structure, subjected to a seismic action characterized by a specific response spectrum, that is able to show a non linear behaviour.

Once found the latter coefficient, consistent with the initial assumption of constant dissipation along the storeys, a different distribution can be useful, especially in the case of tall structures where the relative velocity at each storey can be very different. It consists in the assessment of the dissipation parameter C^* for all the n storeys, that is:

$$C^* = nC \tag{13}$$

redistributed in agreement to a different criterium, proportional to the storey shear, obtained by using the distribution coefficient

$$S_i = \frac{\frac{m_i}{\phi_{1i}}}{\sum_{i=1}^{n} \frac{m_i}{\phi_{1i}}} \tag{14}$$

Finally, to pass from the linear coefficient to the non linear one, the formula proposed in Code FEMA 273 and 274 is used, that is:

$$C_{nl} = \frac{C_l \cdot \left(\left|\dot{x}\right|_{\max}\right)^{1-\alpha}}{\lambda};\ \lambda = \frac{\left[2^{2+\alpha} \cdot \Gamma^2\left(1+\frac{\alpha}{2}\right)\right]}{\pi \cdot \Gamma\left(2+\alpha\right)} \tag{15}$$

where $\left|\dot{x}\right|_{\max}$ is the maximum absolute value of the damper velocity.

4 DESIGN STRATEGY VALIDATION

The FVDs' design strategy reliability is proposed in a probabilistic sense by observing the behaviour of three different benchmark structures: two of them characterized by a plane behavior, coherent with the initial assumptions, and one characterized by an irregular-in plan behaviour (Fig. 1), that do not satisfy the assumed hypothesis. Thereby they are representative of low-rise plane and in-plan irregular structures and mid-rise plane structures.

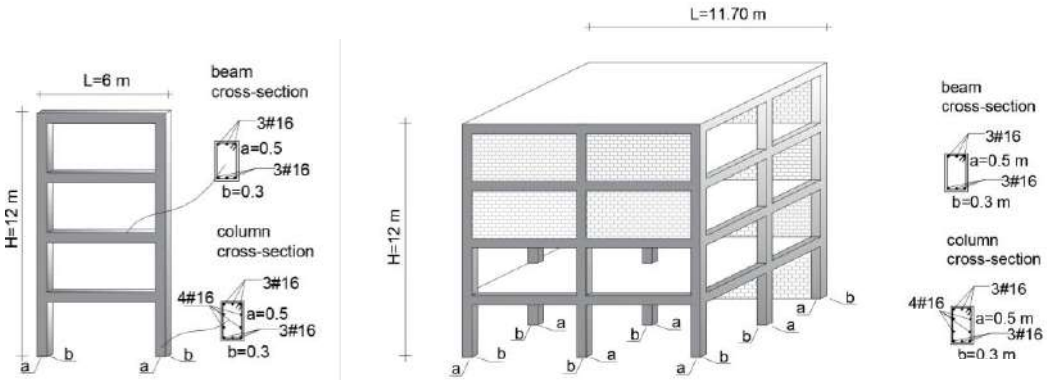

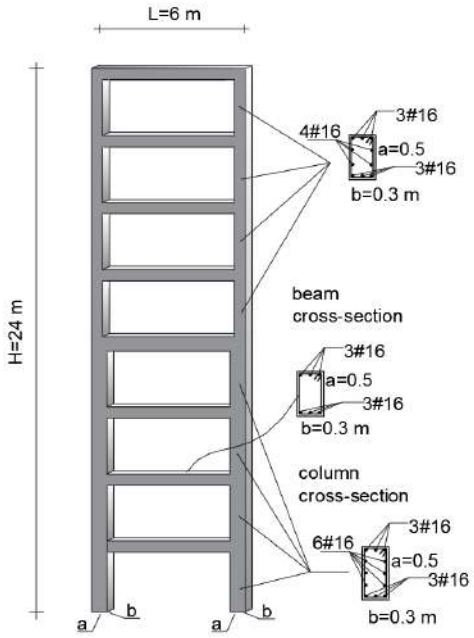

Fig. 1 - Benchmark models: a) plane low-rise structure; b) irregular structure; c) plane mid-rise structure

The four-storey structure stands for low-rise buildings regular in both plane and elevation, while the eight-storey structure stands for mid-rise buildings with the same regularity, assumption on which the proposed strategy is based. On the contrary in the third benchmark structure this assumption has been removed: non-symmetrical infills, producing a strong in-plane irregularity, have been inserted (equivalent pin-jointed diagonal struts, using a linear, indefinite elastic material).

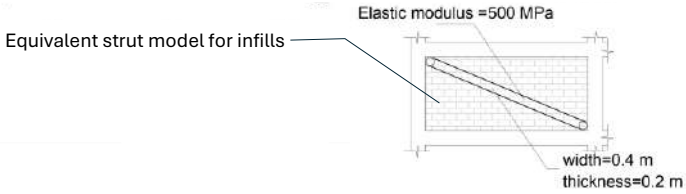

Fig. 2 – Infills equivalent model

Each structural model has been subjected to two levels, 0.7 and 0.5, obtained once the response spectrum has been assigned, of the nominal capacity-demand ratio (C/D) in terms of top displacements, only after that a preliminary pushover analysis for each of the benchmark structures have been performed obtaining the bilinear base shear-top displacement (Fig. 3). The non linear behaviour is expressed through cross section shown in Fig. 1, assumed as fiber section and the materials showing the following constitutive law:

- for concrete Mander (backbone) model and Takeda hysteresis model for cyclic behaviour (f_{cc} 20 MPa, f_2 10.4 MPa; ε_{cc} 0.0013, ε_{cu} 0.005);
- for steel Kinematic hysteresis model for cyclic behaviour (f_{sy} 450 MPa, f_{su} 530 MPa; ε_{sy} 0.0021, ε_{su} 0.675)

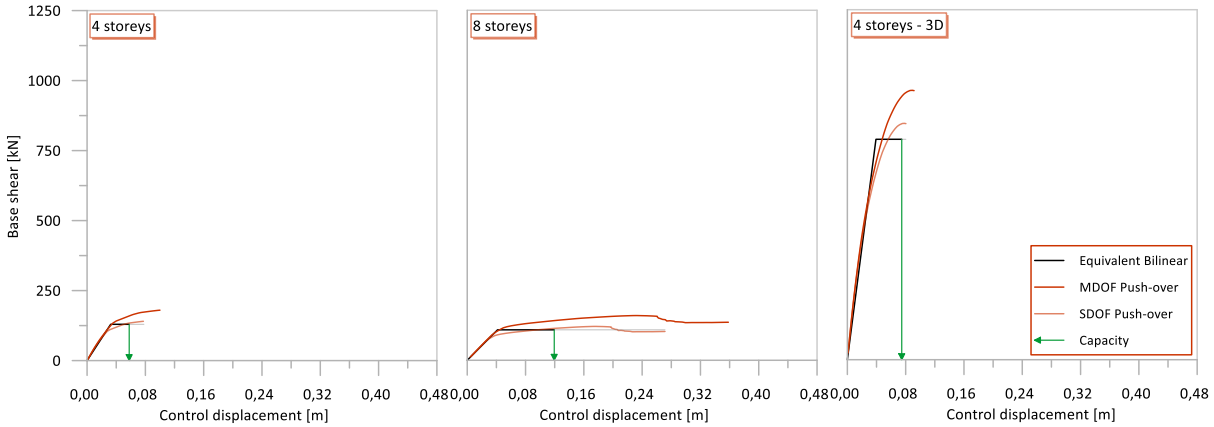

Fig. 3 - Benchmark models' MDOF, SDOF and Bilinear structural responses

In Fig. 4 and Fig. 5 are shown the ADRS used to obtain the capacity-demand ratios and the equivalent force-displacement bilinear curves for each benchmark structure.

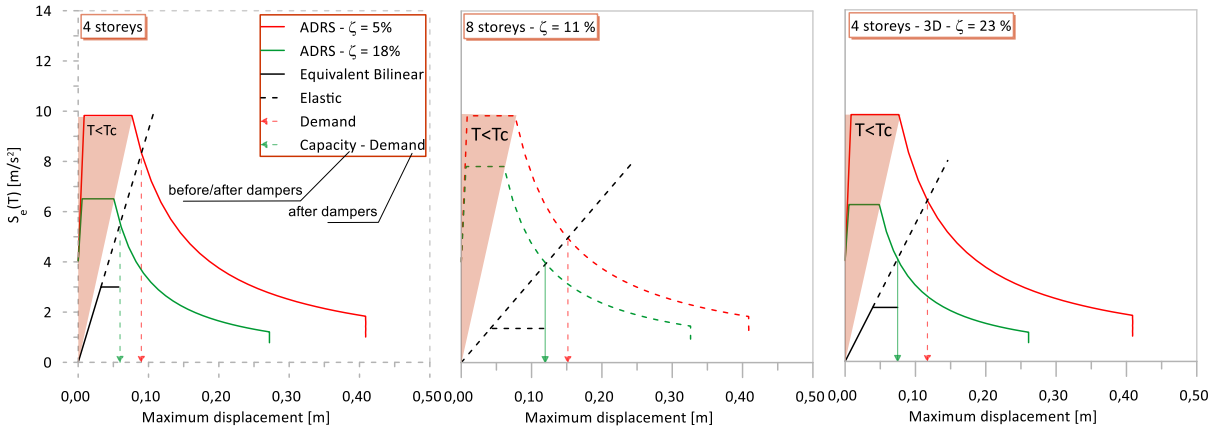

Fig. 4 – ADRS with and without (ζ=5%) fluid viscous dampers (PGA=0.41g), mass normalized bilinear structural responses

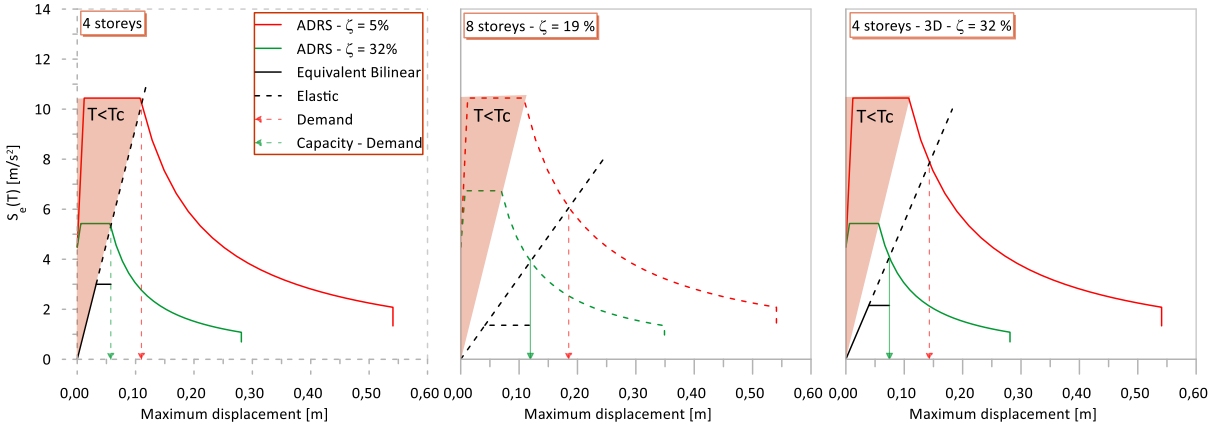

Fig. 5 - ADRS with and without (ζ=5%) fluid viscous dampers (PGA=0.46g), mass normalized bilinear structural responses

Bilinear structural responses and the response spectra are mass normalized for an easier comparison. It is possible to notice that each model is characterized by a fundamental period

.

50

.

.

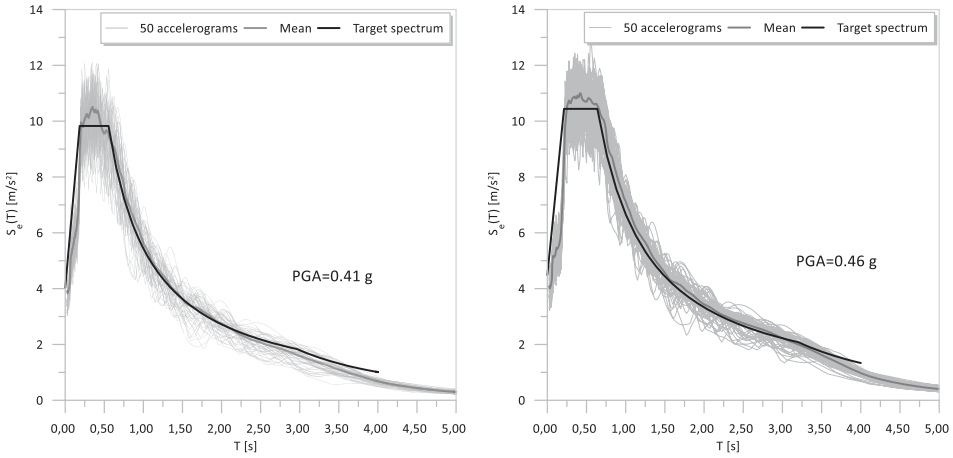

. 6

1

ζ . 7 8 . 4 . 5

α=0.15.

. 1

0.41 0.46.

1 ζ corresponding FVDs' parameters

ζ	$\left[kN \cdot \frac{s}{m}\right]$	$\left[kN \cdot \left(\frac{s}{m}\right)^{0.15}\right]$	$\left[kN \cdot \frac{s}{m}\right]$	$\left[kN \cdot \left(\frac{s}{m}\right)^{0.15}\right]$			
4 *Storeys*							
1 / 27	84 / 828	70 / 149	7 8 / 1590	184 / 97	1 4 / 286	/ 71	84
8 *Storeys*							
6 / 14	17 / 740	9 / 91	9 9 / 2192	114 / 266	115 / 269	14 /	78
4 *Storeys – D*							
18 / 27	840 / 1261	1 7 / 206	1614 / 2421	40 / 605	26 / 95	65 / 99	79

.

In Table 2, mean and standard deviation of the capacity-demand ratios are inserted for comparison, first value is represented of a C/D ratio equal to 0.7 and the second one of a C/D ratio equal to 0.5.

Table 2 - Capacity-demand ratios' mean and standard deviation obtained from 50 dynamic analyses.

	Capacity/Demand	
	Mean	Standard Deviation
4 *Storeys*		
ID - Inherent Damping (5%)	0,625 / 0,485	0,071 / 0,059
AID – Additional Inherent Damping	1,338 / 1,585	0,182 / 0,180
ALD - Uniform Distribution	1,288 / 1,52	0,237 / 0,267
ANLD – Uniform Distribution	1,700 / 3,030	0,384 / 0,641
ALD – Storey Shear Distribution	1,344 / 1,585	0,191 / 0,179
ANLD – Storey Shear Distribution	1,814 / 3,459	0,380 / 0,697
8 *Storeys*		
ID - Inherent Damping (5%)	0,742 / 0,461	0,330 / 0,156
AID – Additional Inherent Damping	1,085 / 0,891	0,368 / 0,359
ALD - Uniform Distribution	0,976 / 0,696	0,374 / 0,336
ANLD – Uniform Distribution	1,082 / 0,700	0,395 / 0,398
ALD – Storey Shear Distribution	1,139 / 1,103	0,303 / 0,240
ANLD – Storey Shear Distribution	1,300 / 1,290	0,209 / 0,202
4 *Storeys* − 3*D*		
ID - Inherent Damping (5%)	0,812 / 0,656	0,103 / 0,098
AID – Additional Inherent Damping	1,348 / 1,299	0,246 / 0,226
ALD - Uniform Distribution	1,297 / 1,239	0,240 / 0,216
ANLD – Uniform Distribution	1,427 / 1,429	0,332 / 0,336
ALD – Storey Shear Distribution	1,350 / 1,300	0,255 / 0,239
ANLD – Storey Shear Distribution	1,511 / 1,549	0,353 / 0,376

In Fig. 7 the capacity-demand distributions are inserted.

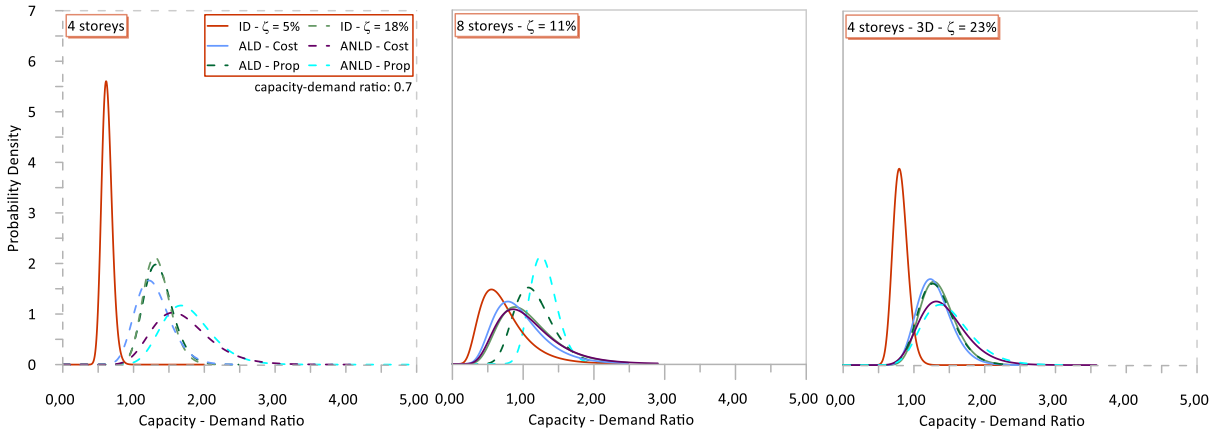

Fig. 7 - Capacity-demand ratio probability density distributions with and without additional damping (ID-ζ=5%: original structure with inherent damping 5%; ID-ζ=18% /11% /23%: structure with inherent damping 18% /11% /23%; ALD-Cost: linear dampers uniformly distributed along the storeys; ANLD-Cost: nonlinear dampers uniformly distributed along the storeys; ALD-Prop: linear dampers distributed according to the storey shear; ANLD-Prop: nonlinear dampers distributed according to the storey shear).

It can be immediately seen how non linear dampers, constant or distributed along the storeys, are the more effective ones among the analyzed types: in the case of mid-rice structures a non uniform distribution returns the best results. Also, considering the limitation of the pushover analysis, it is clear that the most frequent value of capacity-demand ratio in the case of structure without additional damping is not exactly equal to the one from pushover analysis and it is correlated to what this analysis really returns: a range for the capacity-demand ratio. In

Fig. 8 the cumulative density functions are shown.

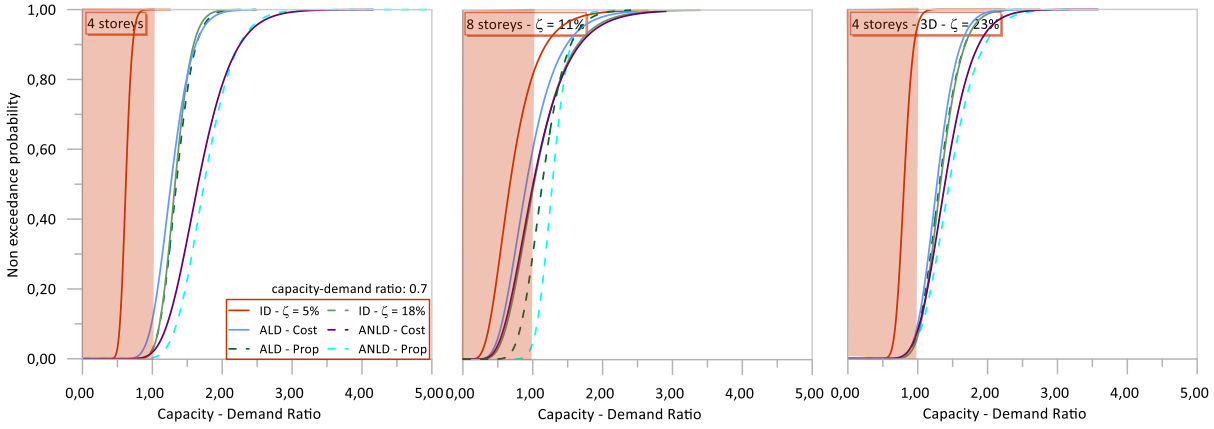

Fig. 8 - Capacity-demand ratio cumulative probability distributions with and without additional damping (legend in caption of Fig. 7)

In the previous sections, during the design stage, the additional damping has been considered as inherent damping. Once found the dissipation coefficient, with the installation of the FVDs, the additional damping is simulated as a concentrated damping at each storeys. In these results it is possible to observe that there is a really small difference between the probability distribution of the capacity demand ratios in the case of additional damping as inherent damping and additional damping as concentrated damping by fluid viscous dampers.

Non uniform distribution is more appropriate for mid-rice structure, remaining effective as the uniform one in case of low-rice structures, regular or not regular in plan. In the latter two cases also it is worth underlining a higher scatter of the capacity-demand ratio of the structures equipped with FVD with respect to the structure in the original state, situation that does not happen in the case of mid-rise structures. This is a consequence of a higher scatter of the results of the capacity-demand ratio in the case of mid-rise structures in the original state.

Hereinafter, in Figs. Fig. 9 and Fig. 10, the results obtained for an initial nominal capacity-demand ratio equal to 0.5 are presented, providing results not different from those obtained in the case of a capacity-demand ratio equal to 0.7.

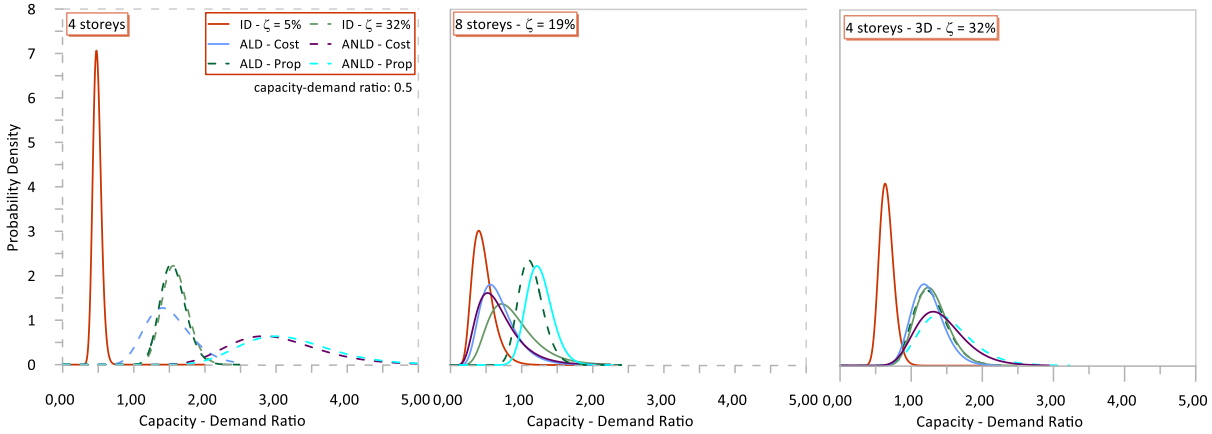

Fig. 9 - Capacity-demand ratio probability density distributions with and without additional damping (ID-ζ=5%: original structure with inherent damping 5%; ID-ζ=32% /19% /32%: structure with inherent damping 32% /19% /32%; ALD-Cost: linear dampers uniformly distributed along the storeys; ANLD-Cost: nonlinear dampers uniformly distributed along the storeys; ALD-Prop: linear dampers distributed according to the storey shear; ANLD-Prop: nonlinear dampers distributed according to the storey shear).

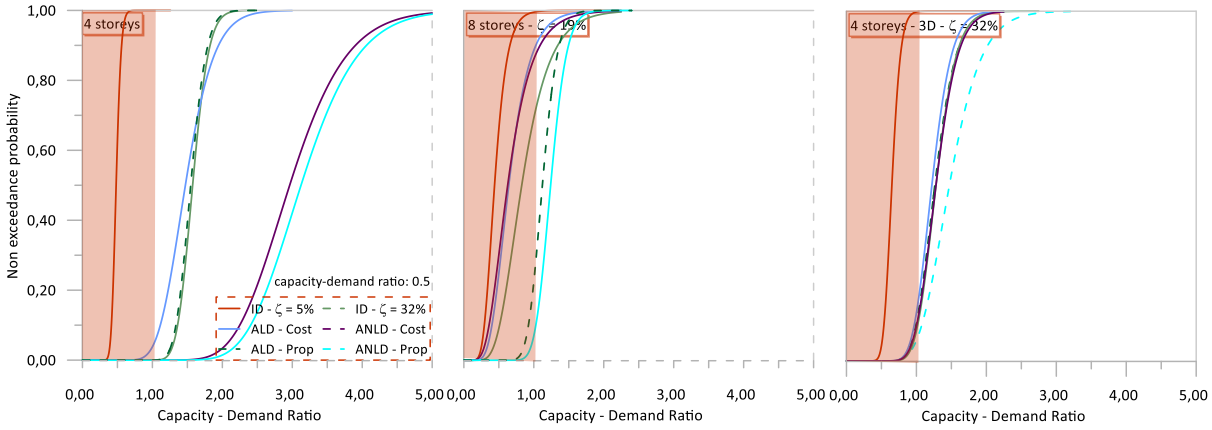

Fig. 10 - Capacity-demand ratio cumulative probability distributions with and without additional damping (legend in caption of Fig. 9)

5 CONCLUSIONS

Considering what was proved in previous sections, it is possible to name FVDs among the most effective seismic protection systems for existing buildings. It is worth underlying that the additional amount of energy dissipation capability adds to the natural capability of structural systems to dissipate through inherent viscosity and hysteresis mechanisms. In this field the proposed strategy is a novelty since a simplified strategy for reinforced concrete framed structures exhibiting a non linear behaviour was missing. This approach starts from a compar-

ison between capacity and demand of a system subjected to a particular earthquake, using the N2 method, and, considering the correlation between indefinitely linear systems and elastic-plastic systems, finds the exact amount of additional dissipation.

The procedure reliability has been valued through a probabilistic assessment and the results obtained have come into some important considerations:

- The three benchmark models show a 95% of probability of having a sufficient capacity demand ratio, higher than 1;
- Non linear dampers are more effective than linear ones, especially if distributed along the storeys;
- Non uniform distribution is more appropriate for mid-rice structure, remaining effective as the uniform one in case of low-rice structures, regular or not regular in plan;
- The initial assumptions do not affect the probability of success since also the benchmark models that are not consistent with the simplifications reach a capacity demand ratio higher than 1.

ACKNOWLEDGMENTS

This study was carried out within the RETURN Extended Partnership and received funding from the European Union Next-GenerationEU (National Recovery and Resilience Plan – NRRP, Mission 4, Component 2, Investment 1.3 – D.D. 1243 2/8/2022, PE0000005)

REFERENCES

[1] Federal Emergency Management Agency (FEMA) and American Society of Civil Engineers (ASCE). Prestandard and commentary for the seismic rehabilitation of buildings. Report FEMA-356, Washington, DC, November 2000.

[2] N. Impollonia, A. Palmeri, Seismic performance of buildings retrofitted with nonlinear viscous dampers and adjacent reaction towers. *Earth Eng Struct Dyn*, **47(5)**, 1329–1351, 2018.

[3] S. Wang, S.A. Mahin, High-performance computer-aided optimization of viscous dampers for improving the seismic performance of a tall building. *Soil Dyn Earth Eng*, **113**, 454–461, 2018.

[4] X. Liu, W. Wang, J. Li, Full-Scale Shaking Table Tests and Numerical Studies of Structural Frames with a Hybrid Isolation System. *Eng Struct*, **292**, 116545, 2023.

[5] R. Ullah, M. Vafaei, S.C. Alih, A. Waheed, A Replaceable Sandwiched Metallic Fuse Damper for Seismic Protection of Braced Frames. *Eng Struct*, **298**, 117072, 2024.

[6] G. Terenzi, Energy-Based Design Criterion of Dissipative Bracing Systems for the Seismic Retrofit of Frame Structures. *Appl Sci*, **8**, 268, 2018.

[7] E. Parcianello, C. Chisari, C. Amadio, Optimal Design of Nonlinear Viscous Dampers for Frame Structures. *Soil Dyn Earth Eng*, **100**, 257–260, 2017.

[8] Y.X. Hui, L.S. Li, H. Cheng, Y.J. Zhang, D.S. Wang, Seismic Mitigation of Continuous Girder Bridges Equipped with U-Shaped Stainless Steel Dampers under near-Fault Earthquake Excitations, *Struct*, **58**, 105597, 2023.

[9] X. Xu, X. Chen, H. Hu, X. Zhou, M. Cheng, L. Sun, X. Li, Energy Dissipation and Seismic Response Reduction System for High-Speed Railway Bridges Based on Multiple Performance Requirements. *Eng Struct*, **307**, 117919, 2024.

[10] J. Fu, S. Wan, P. Zhou, J. Shen, M. Loccufier, K. Dekemele, Effect of Magnetic-Spring Bi-Stable Nonlinear Energy Sink on Vibration and Damage Reduction of Concrete Double-Column Piers: Experimental and Numerical Analysis. *Eng Struct*, **303**, 117517, 2024.

[11] J. Li, L. Xu, Seismic Performance Improvement of Continuous Rigid-Frame Bridges with Hybrid Control System under near-Fault Ground Motions. *Soil Dyn Earth Eng*, **168**, 107858, 2023.

[12] K.V. Sharma, V. Parmar, L. Gautam, S. Choudhary, J. Gohil, Modelling Efficiency of Fluid Viscous Dampers Positioning for Increasing Tall Buildings' Resilience to Earthquakes Induced Structural Vibrations. *Soil Dyn Earth Eng*, **173**, 108108, 2023.

[13] T. Guo, J. Xu, W. Xu, Z. Di, Seismic Upgrade of Existing Buildings with Fluid Viscous Dampers: Design Methodologies and Case Study. *J Perform Constr Facil*, **29**, 04014175, 2015.

[14] M.D. Symans, F.A. Charney, A.S. Whittaker, M.C. Constantinou, C.A. Kircher, M.W. Johnson, R.J. McNamara, Energy Dissipation Systems for Seismic Applications: Current Practice and Recent Developments. *J Struct Eng*, **134**, 3–21, 2008.

[15] M.F. Ferrotto, L. Cavaleri, Variable Friction Dampers (VFD) for a modulated mitigation of the seismic response of framed structures: Characteristics and design criteria. *Prob Eng Mechs*, **70**, 103375, 2022.

[16] M.F. Ferrotto, M. Di Paola, L. Cavaleri, Seismic behavior of structures equipped with variable friction dissipative (VFD) systems. *Bull Earthq Eng*, **19(11)**, 4623–4639, 2021.

[17] L. Cavaleri L, F. Di Trapani, M.F. Ferrotto, Experimental determination of viscous damper parameters in low velocity ranges. *Int J Earthq Eng*, **34(2)**, 64 – 74, 2017.

[18] D. De Domenico, G. Ricciardi, I. Takewaki, Design Strategies of Viscous Dampers for Seismic Protection of Building Structures: A Review. *Soil Dyn Earth Eng*, **118**, 144–165, 2019.

[19] S.S. Ijmulwar, S.K. Patro, Seismic Design of Reinforced Concrete Buildings Equipped with Viscous Dampers Using Simplified Performance-Based Approach. Struct, 61, 106020, 2024.

[20] S. Fajfar, *The Story of the N2 method*. IAEE, 2021.